γ-ray measurements in fast-neutron-induced reactions on ^{203}Tl

N. Fotiades,* R. O. Nelson, and M. Devlin
Los Alamos National Laboratory, Los Alamos, New Mexico 87545, USA

(Received 10 February 2020; accepted 21 May 2020; published 8 June 2020)

Background: Fast-neutron-induced reactions can be used to characterize reaction mechanisms, investigate nuclear structure, and impose constraints on nuclear models. Because of the difficulty in predicting such effects, experimental data are important to constrain models. Thallium isotopes located close to the doubly magic ^{208}Pb nucleus are important for comparison with shell-model calculations.
Purpose: Study the population of excited states in ^{203}Tl and lighter isotopes in such reactions.
Methods: γ-ray cross sections were measured. The data were taken by using the Germanium Array for Neutron-Induced Excitations spectrometer. The pulsed neutron source of the Los Alamos Neutron Science Center's Weapons Neutron Research facility provided neutrons in the energy range from 1 to 300 MeV. The time-of-flight technique was used to determine the incident neutron energies.
Results: Cross sections for emission of several γ rays in 20 reaction channels were determined. Candidates for the intruder $9/2^-$ state in ^{203}Tl, from the odd proton in the $h_{9/2}$ orbital, and the first 5^+ states in ^{202,204}Tl, from admixture of configurations, were identified.
Conclusions: The excitation energy of the candidate $9/2^-$, $\pi h_{9/2}$ state is in good agreement with the theoretical prediction from a semi-empirical weak-coupling model and its half-life is in the range of tens of nanoseconds. The feeding of a previously known isomer in ^{202}Tl exhibits similarities with the feeding of other isomers in this mass region.

DOI: 10.1103/PhysRevC.101.064608

I. INTRODUCTION

Fast-neutron-induced reactions are of interest to basic and applied nuclear physics. For basic nuclear physics, fast-neutron-induced reactions can be used to characterize reaction mechanisms and impose constraints on nuclear models. Fast-neutron-induced reactions populate low-lying excited states; hence, in the case of closed- or near-closed-shell nuclei provide excellent opportunities to study specific orbitals of the nucleus.

The study of excited states in thallium isotopes located close to the doubly magic ^{208}Pb nucleus is important for comparison with shell-model calculations in the lead region. Moreover, these isotopes are good candidates to study the polarizing effect of the high-j intruder orbitals, such as the $\pi h_{9/2}$, $\pi i_{13/2}$, and $\nu i_{13/2}$ orbitals, on the shape of nuclei which are otherwise near spherical at their ground states. In the shell-model calculations in this mass region, from early calculations in Ref. [1] to recent calculations in Refs. [2,3], the $\pi h_{9/2}$ orbital is usually truncated from the calculations, due to very large configurations. As a result, there exist no shell-model predictions for the intruder $9/2^-$ states, from the odd proton occupying the $h_{9/2}$ orbital, in Tl isotopes close to the doubly magic ^{208}Pb nucleus. Luckily, a semi-empirical weak-coupling description of intruder states was introduced in Ref. [4] that includes the $\pi h_{9/2}$ intruder states in this mass region. This model is based on a simple semi-empirical formalism where all the parameters of the model can be extracted from experiment in a self-consistent manner and seems to be valid throughout the periodic table. In the odd-mass Tl isotopes the lowest intruder states are the $9/2^-$ isomers, from the odd proton occupying the $h_{9/2}$ orbital. These states are known from ^{181}Tl [5] up to ^{201}Tl [6], have a less than 1 MeV excitation energy in all cases, and half-lives varying from milliseconds to seconds. The shell-model calculations [1–3] provide no results for the intruder $\pi h_{9/2}$ states; however, the results of the calculations in Ref. [4] successfully reproduce the experimental excitation energies of the known $9/2^-$ isomers (see Fig. 2 in Ref. [4]). Moreover, the latter calculations predict a rapid increase in the excitation energy of the $9/2^-$, $\pi h_{9/2}$ states, starting with ^{203}Tl, as the neutron $N = 126$ shell fills up. The predictions of the model in Ref. [4] for ^{203,205}Tl together with the systematics of the low-lying states in odd-mass Tl isotopes from ^{195}Tl [7] to ^{205}Tl [8] are shown in Fig. 1. The effect of an increase in excitation energy of the $9/2^-$, $\pi h_{9/2}$ state in ^{203}Tl would be twofold. First, the $9/2^-$ state becomes off-yrast; in ^{203}Tl the prediction for its excitation energy at $\approx$1500 keV is now higher than the previously known [11] $9/2^+$ and $11/2^-$ states at 1217.64 and 1449.63 keV, respectively; hence, its population becomes weaker compared with the lighter odd-mass Tl isotopes, rendering its experimental observation more difficult. Moreover, with the previously known 1073.95 keV, $7/2^+$ state [11] below it, an $E1$ transition toward this state is now possible, drastically reducing the expected half-life of the $9/2^-$, $\pi h_{9/2}$ state.

The location of the $9/2^-$, $\pi h_{9/2}$ states in the heavier odd-mass Tl isotopes was unknown. One of the goals of the

*fotia@lanl.gov

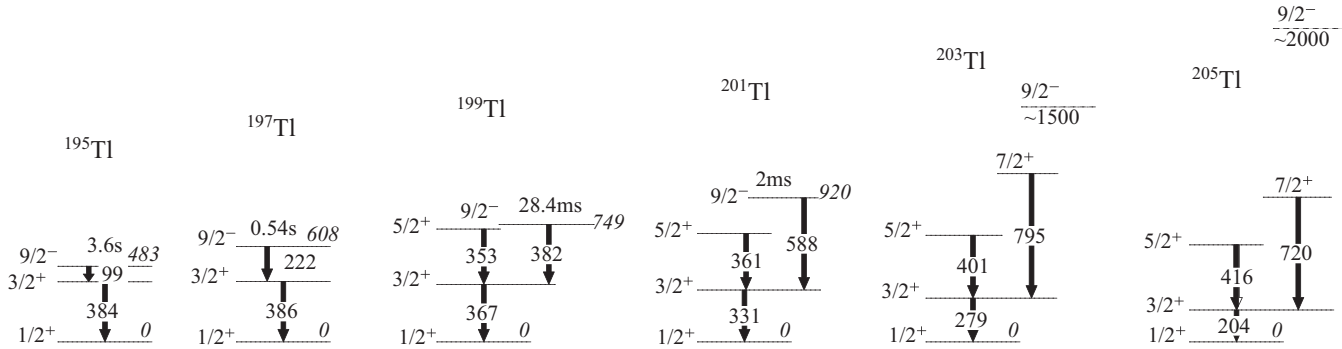

FIG. 1. Partial level schemes of odd-mass Tl isotopes [6–11] and the prediction from Ref. [4] for the $9/2^-$ states in ^{203,205}Tl. All γ-ray and level energies are in keV. We note here that the predictions from Ref. [4] for the $9/2^-$ states in ^{195,197,199,201}Tl (not shown) are in excellent agreement with the experimentally obtained excitation energies included in the present figure.

present experiment was to locate the $9/2^-$, $\pi h_{9/2}$ state in ^{203}Tl and compare the excitation energy with that predicted by the model in Ref. [4]. The $(n, n'\gamma)$ reaction channel used here has the best chance to populate a state expected to be off-yrast because the (n, n') reaction is highly unselective. Hence, it is expected to populate all low-spin states, such as, for instance, in Ref. [12] where all known levels in ^{56}Fe up to 3.6 MeV excitation energy were observed with the (n, n') reaction. A second goal was to obtain partial γ-ray cross sections for as many transitions and reaction channels as possible. Such results provide useful lower limits on the population of states and, combined with model calculations, can give a good estimate of the total population, and more accurate calculations of effective activation cross sections can be made.

II. EXPERIMENT

The experiment was performed at the Los Alamos Neutron Science Center Weapons Neutron Research (LANSCE WNR) facility [13,14]. The γ rays produced in the bombardment of the ^{203}Tl target by neutrons were observed with the Germanium Array for Neutron-Induced Excitations (GEANIE) spectrometer [15]. GEANIE was located 20.34 m from the WNR spallation neutron source on the 60R (60°-Right) flight path. The neutrons were produced in a ^{nat}W spallation target driven by an 800 MeV proton beam with a time structure that consists of 775-μs-long "macropulses," with each macropulse containing subnanosecond-wide "micropulses," spaced every 1.8 μs. The energy of the neutrons was determined by using the time-of-light technique. GEANIE was comprised of 11 Compton-suppressed planar Ge detectors (low-energy photon spectrometers, LEPS), nine Compton-suppressed coaxial Ge detectors and six unsuppressed coaxial Ge detectors. In this setup, half-lives for transitions observed can be extracted from the beam-off data (data obtained between macropulses), provided that the half-lives of the states emitting them are within a range of microseconds to a few milliseconds.

The target consisted of a polystyrene capsule, 2.3 cm in diameter and 0.5 cm thick, containing 2.2 grams of Tl oxide powder, 97.0% enriched in ^{203}Tl. The Tl powder was tightly encapsulated in the thin-walled capsule with an inner diameter of 2.2 cm. The end faces of the sample disk were normal to the neutron beam. During three days of the experiment, out of a total of twenty days, two natural Fe foils, 165 mg/cm^2 thick in total, were placed in front of the ^{203}Tl target so that the known cross section at $E_n = 14.5$ MeV [16] of the strong 846.8 keV, $2^+ \rightarrow 0^+$ transition of ^{56}Fe, produced in natural Fe from inelastic scattering, could be used to normalize the cross sections obtained in the present experiment.

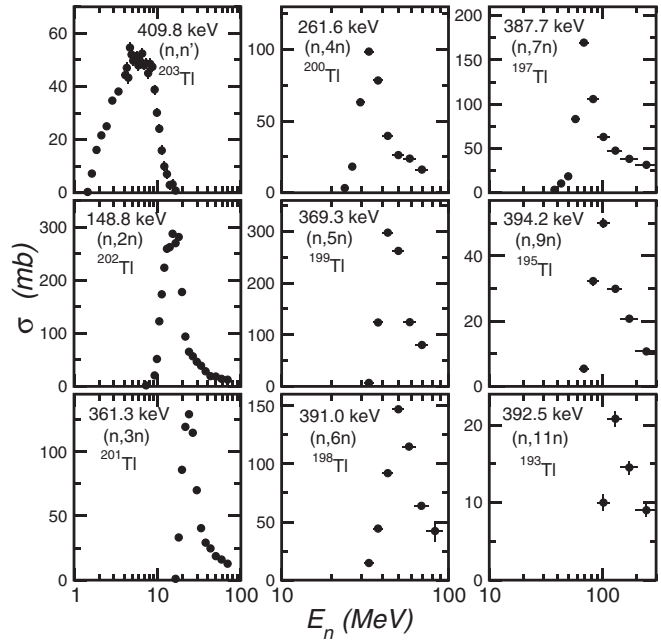

FIG. 2. Examples of absolute partial-cross-section values as a function of incident neutron energy for nine transitions from Tl isotopes observed in the present work. Specifically, the cross sections are shown for the following transitions: 148.8 keV, $(6)^+ \rightarrow 7^+$ of ^{202}Tl [22], 261.6 keV, $6^+ \rightarrow 5^+$ of ^{200}Tl [21], 361.3 keV, $\frac{5}{2}^+ \rightarrow \frac{3}{2}^+$ of ^{201}Tl [6], 369.3 keV, $\frac{11}{2}^- \rightarrow \frac{9}{2}^-$ of ^{199}Tl [10], 387.7 keV, $\frac{11}{2}^- \rightarrow \frac{9}{2}^-$ of ^{197}Tl [9], 391.0 keV, $8^- \rightarrow 7^+$ of ^{198}Tl [20], 392.5 keV, $(\frac{11}{2}^-) \rightarrow (\frac{9}{2}^-)$ of ^{193}Tl [17], 394.2 keV, $\frac{11}{2}^- \rightarrow \frac{9}{2}^-$ of ^{195}Tl [7], and 409.8 keV, $(\frac{9}{2}^-) \rightarrow \frac{7}{2}^+$ assigned to ^{203}Tl in the present work.

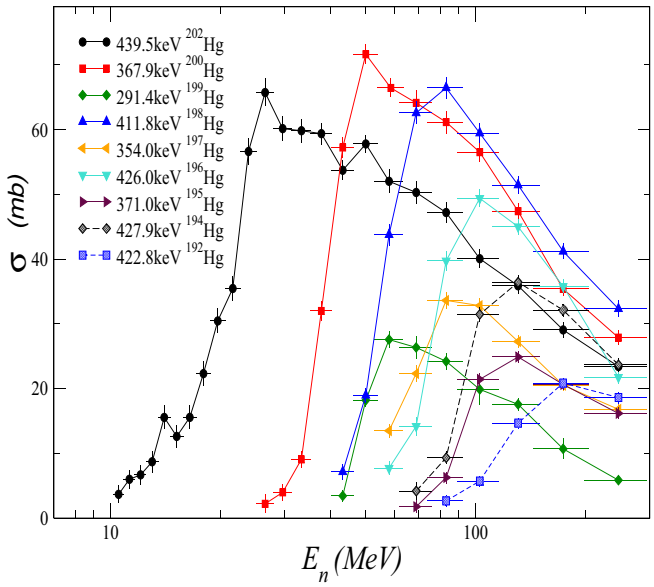

FIG. 3. Examples of absolute partial-cross-section values as a function of incident neutron energy for nine transitions from Hg isotopes observed in the present work. Specifically, the cross sections are shown for the following transitions: 291.4 keV, $(\frac{17}{2}^+) \rightarrow \frac{13}{2}^+$ of ^{199}Hg [10], 354.0 keV, $\frac{17}{2}^+ \rightarrow \frac{13}{2}^+$ of ^{197}Hg [9], 367.9 keV, $2^+ \rightarrow 0^+$ of ^{200}Hg [21], 371.0 keV, $\frac{17}{2}^+ \rightarrow \frac{13}{2}^+$ of ^{195}Hg [7], 411.8 keV, $2^+ \rightarrow 0^+$ of ^{198}Hg [20], 422.8 keV, $2^+ \rightarrow 0^+$ of ^{192}Hg [24], 426.0 keV, $2^+ \rightarrow 0^+$ of ^{196}Hg [19], 427.9 keV, $2^+ \rightarrow 0^+$ of ^{194}Hg [18], and 439.5 keV, $2^+ \rightarrow 0^+$ of ^{202}Hg [23]. Lines are included only to guide the eye.

III. EXPERIMENTAL RESULTS

The cross sections for emission of several γ rays in a total of 20 reaction channels populating isotopes of $^{193-203}$Tl [6,7,9–11,17–22] and $^{192,194-200,202}$Hg [7,9,10,18–21,23,24] were determined in the present experiment. Examples for some of these cross sections are shown in Figs. 2 and 3, while the cross sections for all transitions observed will be presented in a future presentation. Results from the present experiment pertaining to nuclear structure of ^{202}Tl were published in Ref. [22].

The cross sections reported in the present work were corrected for γ-ray attenuation, internal conversion, and contributions from neutrons produced by scattering and reactions in the targets. This is accomplished in the off-line analysis of the data with the help of the MCNPX [25] Monte Carlo radiation transport code, as was described for previous GEANIE experiments (see, for instance, Refs. [26,27] and references therein).

A summary of the states and transitions previously known in ^{203}Tl is given in Ref. [11]. The location of the $9/2^-$ state in ^{203}Tl was unknown before the present experiment. The best candidate observed in the data for this state is a new level at 1483.7 keV excitation energy that deexcites directly to the 1074 keV, $7/2^+$ level, as shown in Fig. 4, via a newly observed 409.8(4) keV transition. This result was briefly reported in an abstract of a meeting in Ref. [28]. The cross section obtained for the 409.8 keV transition is included in Fig. 2.

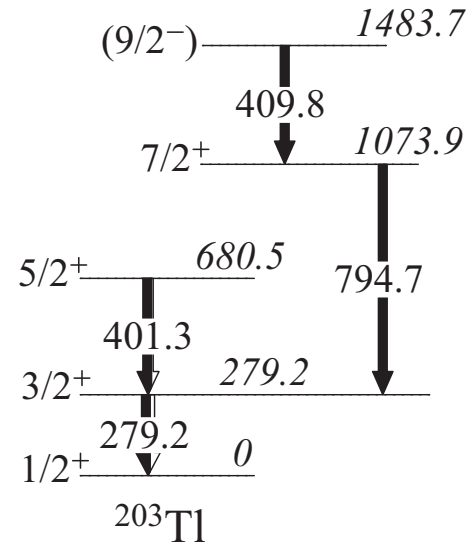

FIG. 4. Partial level scheme of ^{203}Tl as deduced in the present work. All γ-ray and level energies are in keV. The white portion of the arrows indicates the fraction of the decay that is internally converted. The half-life of the 1483.7 keV level is in the range of tens of nanoseconds (see discussion).

The placement of the previously unknown 409.8 keV transition on the level scheme is based on γ-γ coincidence data. The gate on the 409.8 keV transition is shown in Fig. 5. The previously known 279.2 keV, $3/2^+ \rightarrow 1/2^+$ and 794.7 keV, $7/2^+ \rightarrow 3/2^+$ transitions of ^{203}Tl (see Fig. 4) are clearly observed in the gate while the previously known 143.6 keV, $9/2^+ \rightarrow 7/2^+$ transition of ^{203}Tl is not present in this spectrum. The 409.8 keV transition is a weak one; its intensity (the sum over all neutron-induced energies) is 5% that of the 794.7 keV transition and 1.6% that of the 279.2 keV transition. The 409.8 keV was the only new transition assigned to ^{203}Tl in the present experiment.

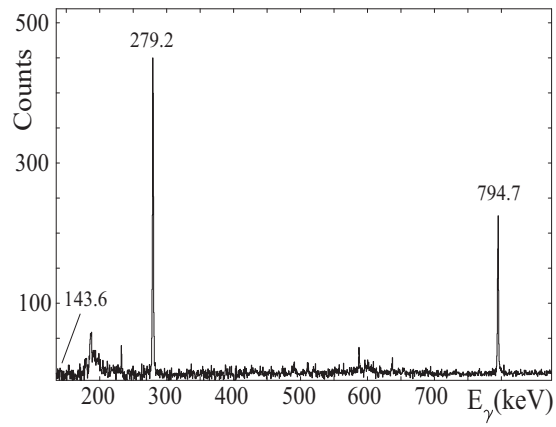

FIG. 5. Gate on the 409.8 keV transition assigned to ^{203}Tl in the γ-γ coincidence data in the present experiment. The 279.2 and 794.7 keV transitions of ^{203}Tl in Fig. 4 are clearly seen while the previously known 143.6 keV transition of ^{203}Tl [11] that feeds the 1073.9 keV state in Fig. 4 is not present in this spectrum.

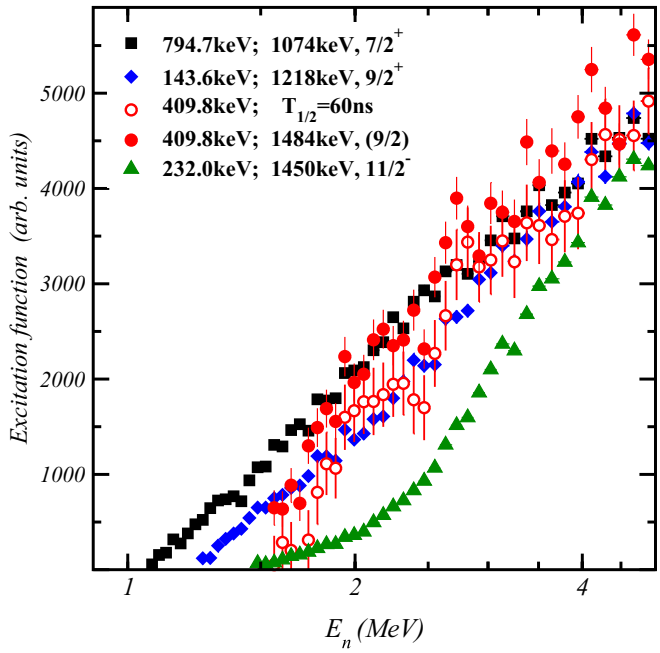

FIG. 6. Excitation functions (up to 5 MeV neutron energy) obtained in the present experiment for three previously known γ rays of ^{203}Tl (143.6, 232.0, and 794.7 keV transitions [11]) from the 1218 (solid diamonds), 1450 (solid triangles), and 1074 keV (solid squares) levels, respectively, and the 409.8 keV transition (solid circles) which is assigned to ^{203}Tl in the present work. The open circles are the results for the 409.8 keV transition shifted assuming a 60 ns half-life for the 1483.7 keV level.

The 409.8 keV transition is observed only in the prompt-γ-ray data and not observed in the beam-off data. Moreover, in the beam-off data no previously known transitions of ^{203}Tl were observed, excluding the presence of longer-lived isomers in this isotope (within the limits of observation of the present experiment and excluding cases of isomers that decay only directly to the ground state). An upper limit for the half-life of the 1483.7 keV state is estimated at 1 μs. Hence, this state, if it is an isomer, is a short-lived one, as opposed to the $9/2^-$ states in the lighter odd-mass Tl isotopes (see Fig. 1). This is mainly because, in the lighter odd-mass Tl isotopes, the first $7/2^+$ states are located at higher excitation energies than the $9/2^-$ states.

IV. DISCUSSION

The excitation function for the 409.8 keV transition is shown in Fig. 6 together with the excitation functions obtained for previously known transitions of ^{203}Tl [11]. From comparison of the excitation functions in Fig. 6, a $9/2$ spin assignment for the 1483.7 keV state can be tentatively suggested. The steeper increase of the excitation function of the 409.8 keV transition compared with that of the 143.6 keV transition (which is emitted by the 1217.64 keV, $9/2^+$ state) in Fig. 6 could be due to the short half-life of the 1483.7 keV state, which affects the shape of the excitation function of the 409.8 keV transition by "misplacing" neutron counts to lower neutron energies in the data (see details given in Ref. [29]). To correct for this "misplacement" of counts the half-life of the emitting state has to be known. In the same figure, a corrected neutron excitation function for the 409.8 keV transition is shown by assuming a half-life of 60 ns for the 1483.7 keV emitting level. By such a correction the neutron excitation function of the 409.8 keV transition approaches that of the 143.6 keV transition which is emitted by a $9/2$ state. Hence, its half-life can be on the order of tens of nanoseconds, as expected for the $\pi h_{9/2}$ state in ^{203}Tl (see earlier discussion in Sec. I). The neutron excitation functions for the previously known 232.0 and 794.7 keV transitions, emitted by a $11/2$ and a $7/2$ state, respectively, are also included in Fig. 6 for comparison and, in both cases, the shape of the neutron excitation function for the 409.8 keV transition is intermediate between the neutron excitation functions for these transitions. From the discussion above it can be suggested that the 1483.7 keV is the best candidate in the present data for the $9/2^-$, $\pi h_{9/2}$ state in ^{203}Tl, with a half-life in the range of tens of nanoseconds.

The semi-empirical weak-coupling model in Ref. [4] predicts the intruder $9/2^-$, $\pi h_{9/2}$ state at $\approx$1500 keV excitation energy in ^{203}Tl. The candidate observed in the present work at 1483.7 keV excitation energy is in excellent agreement with the model prediction. Until the shell-model calculations in this mass region are capable of including the $\pi h_{9/2}$ intruding orbital, the model in Ref. [4] is the only alternative prediction for its location in these nuclei. The excellent agreement between the measurement presented here and the prediction of this model enhances the validity of the model's predictions for ^{205}Tl and ^{207}Tl. Similar data to those presented here were obtained also with GEANIE in fast-neutron-induced reactions on ^{205}Tl [30]. A new 990.5 keV transition can be assigned to ^{205}Tl from these data. However, this transition is relatively weaker than the 409.8 keV observed in the present experiment, and its placement in the ^{205}Tl remains uncertain. If the 990.5 keV transition is placed as feeding the $7/2^+$ state of ^{205}Tl in Fig. 1, it would define a new level at 1914 keV excitation energy which lies very close to a previously known 1916 keV level assigned to ^{205}Tl in a ^{208}Pb(pol p, α) reaction [31] as a $11/2^+$ state [see also the evaluation in Ref. [8] where 1916(3) keV, $(11/2^+, 13/2^+)$, was adopted]. Moreover, there exist more possible decay paths for a $9/2^-$ state at $\approx$2000 keV excitation energy in ^{205}Tl, as predicted in Ref. [4] (see Fig. 1). Hence, the intensities of the transitions involved in such a decay would be less than the intensity observed for the 409.8 keV transition in the present experiment and, most likely, lie below the intensity limit for observation in the GEANIE ^{205}Tl experiment.

The 7^+ isomers in all doubly odd Tl isotopes in this mass region originate from the $(\pi^{-1}s_{1/2} \otimes \nu^{-1}i_{13/2})$ configuration [2,32]. Recently, the systematics of the 7^+ isomers in ^{196,198,200}Tl and of the nearby-located 5^+ isomers, from the $(\pi^{-1}d_{3/2} \otimes \nu^{-1}i_{13/2})$ configuration, was compared with the $13/2^+$ isomers in neighboring odd-mass Pb isotopes in Ref. [32]. This comparison can be extended in the present work to the heavier ^{202,204,206}Tl isotopes. It is expected that the corresponding 5^+ and 7^+ states in ^{202,204}Tl are populated in fast-neutron-induced reactions on stable ^{203,205}Tl isotopes, as was done in the present work and in Ref. [30]. The 922.6 keV state of ^{202}Tl observed in the present work and reported in

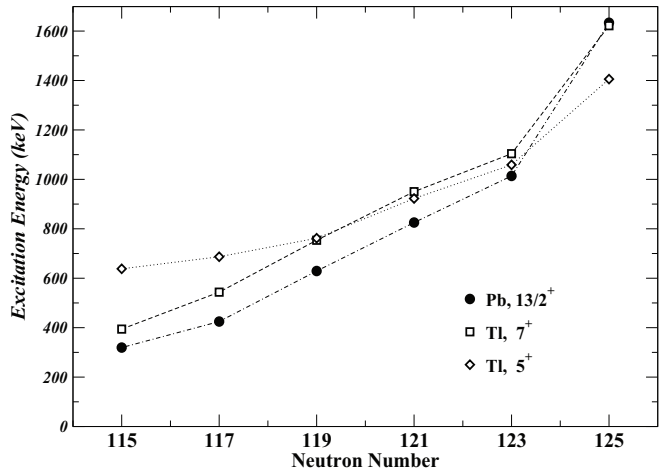

FIG. 7. Systematics of level energies of the $\frac{13}{2}^+$ states in odd-mass Pb isotopes, and the 5_1^+ and 7_1^+ states in doubly odd Tl isotopes. Data taken from Refs. [6,8–11,22,30,32–34].

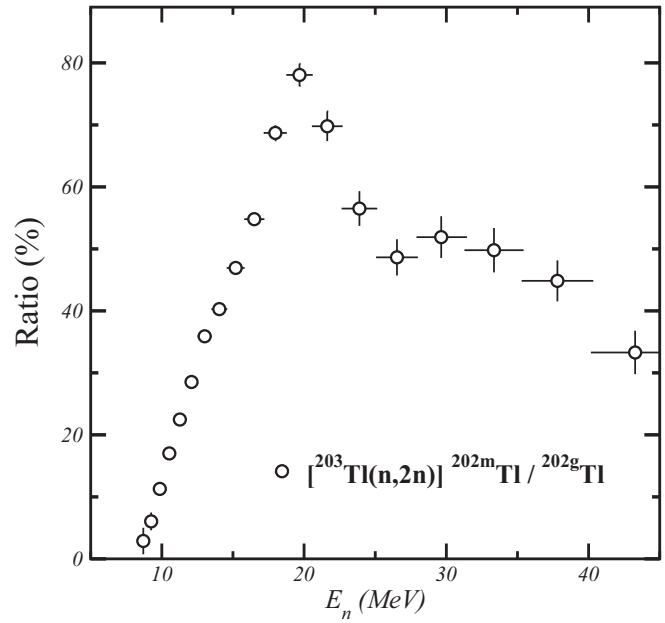

FIG. 8. Ratio of the sum of cross sections for the three transitions feeding directly the 7^+ isomer of ^{202}Tl with the sum of cross sections for the five transitions feeding directly the 2^- ground state of ^{202}Tl in Fig. 2 of Ref. [22].

Ref. [22], and the 1058.8 keV state of ^{204}Tl reported in Ref. [30] are good candidates for the first 5^+ states, based on the expanded systematics shown in Fig. 7. Shell-model calculations for the 1405.47 keV, $(5)^+$ state of ^{206}Tl [33,35] included in Fig. 7 give 77% contribution from the $(\pi^{-1}h_{11/2} \otimes \nu^{-1}p_{1/2})$ configuration, 9% from the $(\pi^{-1}d_{3/2} \otimes \nu^{-1}i_{13/2})$ configuration, and 7% from the $(\pi^{-1}h_{11/2} \otimes \nu^{-1}f_{5/2})$ configuration. All these configurations could contribute to the 5^+ states of ^{202,204}Tl in Fig. 7. The 7^+ states in Fig. 7 follow the general behavior observed for the $13/2^+$ states in odd-mass Pb isotopes, hence, the underlying $(\pi^{-1}s_{1/2} \otimes \nu^{-1}i_{13/2})$ configuration is rather pure for these states, as discussed also in Ref. [32] and supported by shell-model calculations [2]. On the other hand, the possible admixtures of more than one configuration mentioned above for the 5_1^+ states could be the reason for the different behavior observed for these states in Fig. 7. Moreover, the percentage of the admixtures can vary for each isotope, starting with the values listed above for the $(5)^+$ state of ^{206}Tl [33,35] and ending with a purer $(\pi^{-1}d_{3/2} \otimes \nu^{-1}i_{13/2})$ configuration for the 5^+ states of ^{198,200}Tl, as suggested in Ref. [32]. It is noteworthy that the excitation energies proposed in the present work for the 5_1^+ states of ^{202,204}Tl are in very good agreement with the predictions from the shell-model calculations in Ref. [2]. These calculations also reproduce very well the excitation energy of the $(5)^+$ state of ^{206}Tl.

In Fig. 8 the ratio of the sum of cross sections, for three transitions feeding directly the 7^+ isomer of ^{202}Tl (148.8, 389.9, and 601.9 keV transitions) with the sum of cross sections for five transitions feeding directly the 2^- ground state of ^{202}Tl (186.2, 190.0, 312.4, 348.3, and 490.5 keV transitions) in the level scheme in Fig. 2 of Ref. [22], is shown. Thus, this represents the ratio of the experimentally observed part of the ^{203}Tl$(n, 2n)^{202m}$Tl cross section to the experimentally observed part of the ^{203}Tl$(n, 2n)^{202g}$Tl cross section and shows a qualitative picture of the variation in the feeding of the 7^+ isomer with respect to the feeding of the ground state with increasing neutron energy. The population of the isomer increases up to ≈20 MeV neutron energy. The opening of the $(n, 3n)$ reaction channel occurs at about this neutron energy. The $(n, 3n)$ reaction channel is expected to carry away a bigger part of the high-spin component of the strength of the reaction and, hence, it affects more the population of the high-spin 7^+ isomer, leading to a decrease of the ratio in Fig. 8. Similar behavior has been observed in the population of $11/2^-$ isomers in the neighboring stable iridium and gold isotopes [27] as well as in the mass $A \approx 100$ region [36].

The cross sections obtained for the $2^+ \rightarrow 0^+$ Hg γ rays in Fig. 3 can be interpreted as a good approximation of the total production cross sections. Almost all decaying γ cascades in residual even-even nuclei proceed through the lowest $2^+ \rightarrow 0^+$ transition, as has been noted previously at lower reaction energies [37–39]. Hence, these results are relevant for testing reaction models. On the other hand, in the odd-mass and odd-odd isotopes populated in the present work the γ-ray cascades to the ground state proceed through different paths via several low-lying levels, hence, the obtained cross sections for the lowest transitions in these cases represent only a part of the total cross section of the corresponding reaction channels. Indeed, as it can be seen in Fig. 3, the lowest transitions observed for ^{195,197,199}Hg are all feeding previously known $13/2^+$ isomers and their cross sections are weaker than those in the neighboring even-even isotopes.

V. SUMMARY

γ rays emitted in fast-neutron-induced reactions on ^{203}Tl were measured with the GEANIE spectrometer. Partial cross

sections for several transitions were measured for neutron energies 1 MeV $< E_n <$ 300 MeV and reaction channels emitting up to 12 particles. Candidates for the $9/2^-$ intruder state in ^{203}Tl, from the odd proton in the $h_{9/2}$ orbital, and the first 5^+ states in ^{202,204}Tl, from admixture of configurations, are suggested. The excitation energy of the $9/2^-$ state of ^{203}Tl is in excellent agreement with the prediction for intruder states from a semi-empirical weak-coupling model, while the excitation energies of the 5_1^+ states of ^{202,204}Tl follow the excitation energy systematics in doubly odd Tl isotopes up to the neutron closed shell. Moreover, the present data provide new information for partial γ-ray cross sections over a wide neutron-energy range and are valuable as an input for future theoretical calculations on the same or similar reactions. Thus, the present work is important for its contribution to both nuclear reactions and nuclear structure in this mass region.

ACKNOWLEDGMENTS

GEANIE, decommissioned in 2015, was a joint Los Alamos National Laboratory (LANL) and Lawrence Livermore National Laboratory (LLNL) project supported by the U.S. Department of Energy (DOE) in part under Contracts No. W-7405-ENG-36 and DE-AC52-06NA25396 for LANL, and W-7405-ENG-48 and DE-AC52-07NA27344 for LLNL. This work has benefited from use of the LANSCE accelerator facility supported under DOE Contracts No. W-7405-ENG-36 and No. DE-AC52-06NA25396.

[1] A. Covello and G. Sartoris, Nucl. Phys. A **93**, 481 (1967).
[2] H. Jiang, J. J. Shen, Y. M. Zhao, and A. Arima, J. Phys. G **38**, 045103 (2011).
[3] F. I. Sharrad, A. A. Okhunov, H. Y. Abdullah, and H. Abu Kassim, Rom. J. Phys. **58**, 99 (2013).
[4] G. E. Arenas Peris and P. Federman, Phys. Rev. C **38**, 493 (1988).
[5] S.-C. Wu, Nucl. Data Sheets **106**, 367 (2005).
[6] F. G. Kondev, Nucl. Data Sheets **108**, 365 (2007).
[7] Huang Xiaolong and Kang Mengxiao, Nucl. Data Sheets **121**, 395 (2014).
[8] F. G. Kondev, Nucl. Data Sheets **101**, 521 (2004).
[9] Huang Xiaolong and Zhou Chunmei, Nucl. Data Sheets **104**, 283 (2005).
[10] Balraj Singh, Nucl. Data Sheets **108**, 79 (2007).
[11] F. G. Kondev, Nucl. Data Sheets **105**, 1 (2005).
[12] N. Fotiades, R. O. Nelson, and M. Devlin, Phys. Rev. C **81**, 037304 (2010).
[13] P. W. Lisowski, C. D. Bowman, G. J. Russell, and S. A. Wender, Nucl. Sci. Eng. (La Grange Park, IL, US) **106**, 208 (1990).
[14] P. W. Lisowski and K. F. Schoenberg, Nucl. Instrum. Methods Phys. Res., Sect. A **562**, 910 (2006).
[15] J. A. Becker and R. O. Nelson, Nucl. Phys. News **7**, 11 (1997).
[16] R. O. Nelson, N. Fotiades, M. Devlin, J. A. Becker, P. E. Garrett, and W. Younes, AIP Conf. Proc. **769**, 838 (2005).
[17] M. Shamsuzzoha Basunia, Nucl. Data Sheets **143**, 1 (2017).
[18] Balraj Singh, Nucl. Data Sheets **107**, 1531 (2006).
[19] Huang Xiaolong, Nucl. Data Sheets **108**, 1093 (2007).
[20] Huang Xiaolong and Kang Mengxiao, Nucl. Data Sheets **133**, 221 (2016).
[21] F. G. Kondev and S. Lalkovski, Nucl. Data Sheets **108**, 1471 (2007).
[22] N. Fotiades, R. O. Nelson, M. Devlin, and J. A. Becker, Phys. Rev. C **76**, 014302 (2007).
[23] S. Zhu and F. G. Kondev, Nucl. Data Sheets **109**, 699 (2008).
[24] C. M. Baglin, Nucl. Data Sheets **113**, 1871 (2012).
[25] MCNPX User's Manual, Version 2.7.0, edited by X-5 Monte Carlo Team, Los Alamos National Laboratory Controlled Publication, LA-CP-11-00438 (2011).
[26] N. Fotiades *et al.*, Phys. Rev. C **69**, 024601 (2004).
[27] N. Fotiades, R. O. Nelson, M. Devlin, S. Holloway, T. Kawano, P. Talou, M. B. Chadwick, J. A. Becker, and P. E. Garrett, Phys. Rev. C **80**, 044612 (2009).
[28] N. Fotiades, R. O. Nelson, M. Devlin, J. A. Becker, and W. Younes, Bull. Am. Phys. Soc. **51**, No. 6, 90 (2006).
[29] N. Fotiades, P. Casoli, P. Jaffke, M. Devlin, R. O. Nelson, T. Granier, P. Talou, and T. Ethvignot, Phys. Rev. C **99**, 024606 (2019).
[30] N. Fotiades, R. O. Nelson, M. Devlin, and J. A. Becker, Phys. Rev. C **77**, 024306 (2008).
[31] E. Gadioli *et al.*, Phys. Rev. C **43**, 2572 (1991).
[32] Poulomi Roy *et al.*, Phys. Rev. C **100**, 024320 (2019).
[33] F. G. Kondev, Nucl. Data Sheets **109**, 1527 (2008).
[34] F. G. Kondev and S. Lalkovski, Nucl. Data Sheets **112**, 707 (2011).
[35] K. K. Seth, Nucl. Data Sheets **B7**, 161 (1972).
[36] N. Fotiades, M. Devlin, R. O. Nelson, T. Kawano, and J. J. Carroll, Phys. Rev. C **94**, 044608 (2016).
[37] R. B. Day, Phys. Rev. **102**, 767 (1956).
[38] J. R. Huizenga and R. Vandenbosch, Phys. Rev. **120**, 1305 (1960).
[39] R. Vandenbosch and J. R. Huizenga, Phys. Rev. **120**, 1313 (1960).